Paper-Based Origami Triboelectric Nanogenerators and Self-Powered Pressure Sensors

Po-Kang Yang,[†,‡,§,#] Zong-Hong Lin,[†,∥,#] Ken C. Pradel,[†] Long Lin,[†] Xiuhan Li,[†] Xiaonan Wen,[†] Jr-Hau He,[*,§] and Zhong Lin Wang[*,†,⊥]

[†]School of Materials Science and Engineering, Georgia Institute of Technology, Atlanta, Georgia 30332-0245, United States, [‡]Institute of Photonics and Optoelectronics and Department of Electrical Engineering, National Taiwan University, Taipei 10617, Taiwan, [§]Computer, Electrical and Mathematical Sciences and Engineering (CEMSE) Division, King Abdullah University of Science & Technology (KAUST), Thuwal 23955-6900, Saudi Arabia, [∥]Institute of Biomedical Engineering, National Tsing Hua University, Hsinchu 30013, Taiwan, and [⊥]Beijing Institute of Nanoenergy and Nanosystems, Chinese Academy of Sciences, Beijing, China. [#]These authors contributed equally to this work.

ABSTRACT Discovering renewable and sustainable power sources is indispensable for the development of green electronics and sensor networks. In this paper, we present origami triboelectric nanogenerators (TENGs) using paper as the starting material, with a high degree of flexibility, light weight, low cost, and recyclability. Slinky- and doodlebug-shaped TENGs can be easily fabricated by properly folding printer papers. The as-fabricated TENGs are capable of harvesting ambient mechanical energy from various kinds of human motions, such as stretching, lifting, and twisting. The generated electric outputs have been used to directly light-up commercial LEDs. In addition, the as-fabricated TENGs can also serve as self-powered pressure sensors.

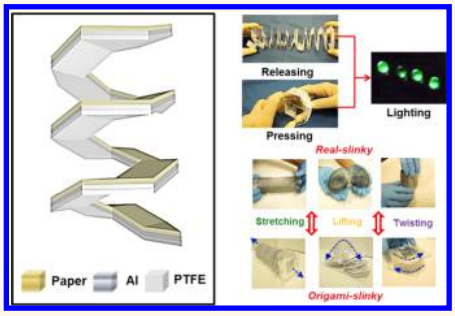

KEYWORDS: origami · green electronics · triboelectric nanogenerators · self-powered sensors

Due to an increasing demand for green electronics, the development of biocompatible and biodegradable devices that can generate power has attracted great attention in recent years.[1] Paper, formed by multiple layers of cellulose fibers, has been recognized as the most environmentally friendly material in the world. In addition, paper possesses the advantages of flexibility, light weight, low cost, and recyclability; once an electronic device is fabricated with or using paper, a broad technological impact will be created in the field of renewable and sustainable energy. Therefore, several attempts have been made in innovating paper-based electronics for energy storage and conversion applications, such as Li-ion batteries,[2] self-powered supercapacitors,[3,4] solar cells,[5,6] and nanogenerators.[7,8]

Mechanical energy, which can be produced from human motions, sounds, and structure vibrations, is probably the most common renewable energy source in our living environment. To effectively convert mechanical energy to electricity, piezoelectric nanogenerators, triboelectric nanogenerators (TENGs), electret generators, and electrostatic generators have been successfully developed and their potentials demonstrated.[9−12] Among them, TENGs have been proven as one of the cost-effective and robust approaches for harvesting ambient mechanical energy.[13−17]

The operating principle of TENG is based on the periodical contact and separation of two different materials that have opposite triboelectric polarities. The contact of two different materials will cause triboelectric charged surfaces. During the motions of contact and separation, potential differences are created, which will contribute to the flow of electrons between the back conductive electrodes and generate electric outputs. Although the operating principle of TENG is simple, there still remain several challenges for the development of TENGs. For instance, conventional TENGs generally work in either contact or sliding modes, which mostly

* Address correspondence to zlwang@gatech.edu, jrhau.he@kaust.edu.sa.

Received for review November 20, 2014 and accepted January 2, 2015.

Published online 10.1021/nn506631t

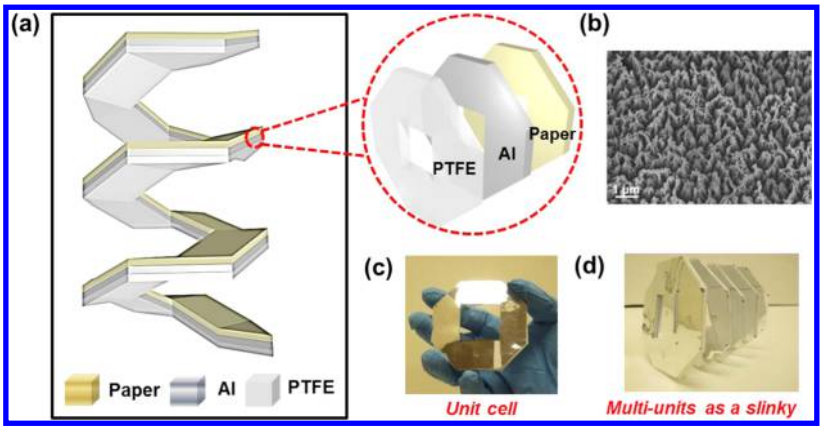

Figure 1. Structure and photographs of a slinky TENG. (a) Schematic diagram of a slinky TENG. (b) SEM image of the etched PTFE surface with nanowire-like structure. (c) Photograph of the unit cell in slinky TENG. (d) Photograph of multiunits in forming a slinky structure.

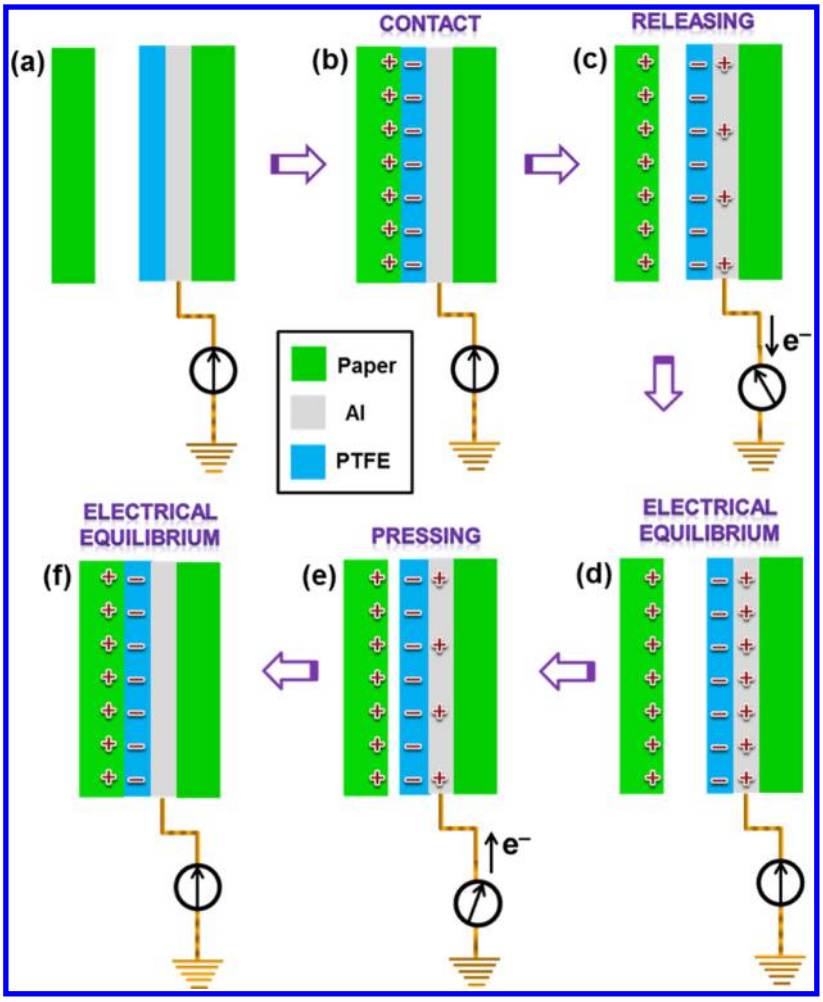

Figure 2. Working mechanisms of the slinky TENG. (a) Original position of two contact surfaces in slinky TENG. (b) External force brings the PTFE thin film and paper into contact, inducing positive triboelectric charges on the paper side and negative charges on the PTFE side. (c) Withdrawal of the force causes a separation. Electrons flow out of the aluminum foil. (d) Charge distribution of the slinky TENG after electrical equilibrium. (e) Electrons are driven back as the force is applied again, reducing the inductive charges on the aluminum foil. (f) Charge distribution of the slinky TENG reaches a new equilibrium.

rely on a single-direction trigger. This will limit the application of TENGs in harvesting energy only from specific directions.

To solve the problem, TENGs with integrated structures are strongly desired and have already been demonstrated. For example, a multilayered TENG is

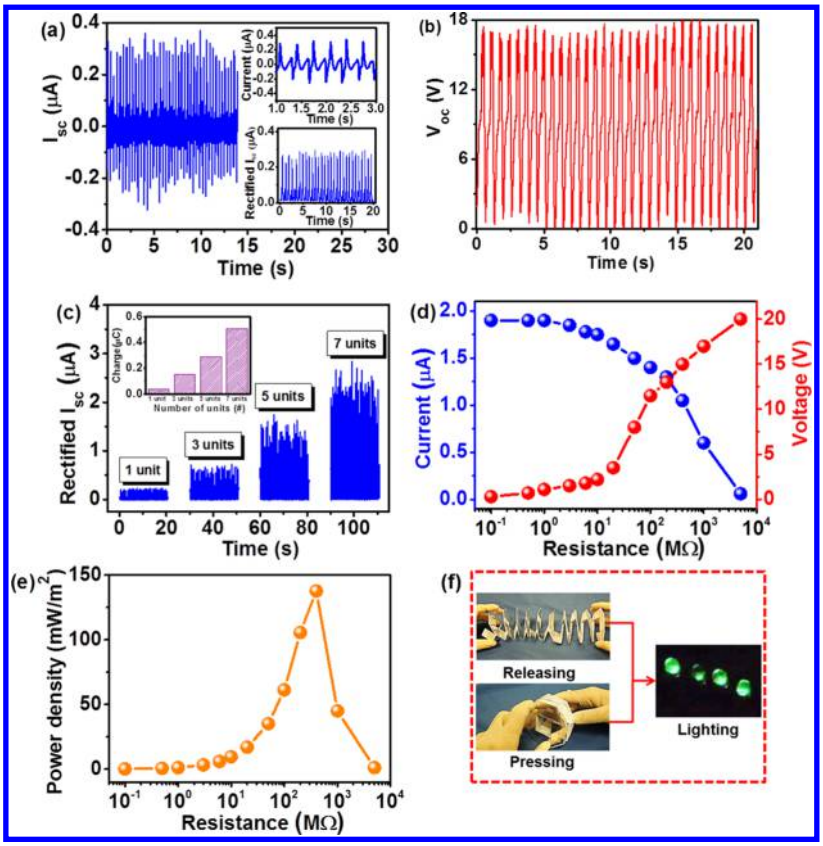

Figure 3. Electrical outputs of the slinky TENG in parallel connections. (a) Short-circuit current (I_{sc}) of the unit cell in the slinky TENG. The enlarged view of six cycles and rectified I_{sc} are also shown as the inset. (b) Open-circuit voltage (V_{oc}) of the unit cell. (c) Rectified I_{sc} of different number of units. The inset shows the transferred charge quantity (ΔQ). (d) Relationship between the output voltage (red)/current (blue) and the resistance of the external loads of the slinky TENG in seven units. (e) Relationship between instantaneous power density and resistance of the external loads of the slinky TENG in seven units. The maximum power density is approximately 0.14 W m^{-2} when the external load is 400 MΩ. (f) Photographs of four commercial green LEDs driven by the slinky TENG. The effective contact area of the slinky TENG is 32 cm^2.

developed in order to scale up the output power density.[16] Moreover, three-dimensional (3D) stacked and rhombic gridding TENGs are also reported to harvest the vibration energy.[18,19]

Regarding paper-based electronics, an origami approach has been recognized as an effective technique to build up structures.[20−22] Through the origami approach, even complicated 3D structures with a high degree of folding can be directly constructed. Scientists have utilized origami in several practical applications, such as light-emitting diodes (LEDs),[23] Li-ion batteries,[24] and biosensors.[25]

In this work, we develop a new type of paper-based TENG with origami configurations for harvesting mechanical energy. The origami approach provides a facile path to fabricate a stacked TENG without expanding the area or complicating the fabrication process. A TENG with slinky shape is developed by connecting seven units in parallel. The output short-circuit current (I_{sc}) and open-circuit voltage (V_{oc}) of the slinky TENG can reach 2 μA and 20 V, respectively. A corresponding instantaneous power density of 0.14 W m^{-2} is obtained at a load resistance of 400 MΩ. The generated electrical output has been demonstrated to directly light up commercial LEDs. We also show the slinky TENG with the advantage of harvesting energy from various kinds of human motions, such as stretching, lifting, and twisting. Furthermore, the slinky TENG can serve as a self-powered pressure sensor to differentiate the weight difference of coins. The doodlebug TENG is also demonstrated to expand the application scope of the origami approach. We believe that these findings will pave the way for future energy harvesting and sensor design, especially for the development of green electronics.

RESULTS AND DISCUSSION

The configuration of the slinky TENG is schematically illustrated in Figure 1a. It is clearly shown that the slinky TENG is composed of three parts, including a paper substrate, polytetrafluoroethylene (PTFE) thin film, and aluminum foil. Figure 1b shows a scanning electron microscopy (SEM) image of the PTFE thin film surface. A uniformly distributed nanowire-like structure can be observed with a dimension about ~700 nm in length and ~70 nm in width. It has been theoretically reported that the charges on the PTFE surface can be retained for years, which guarantees the sustainable

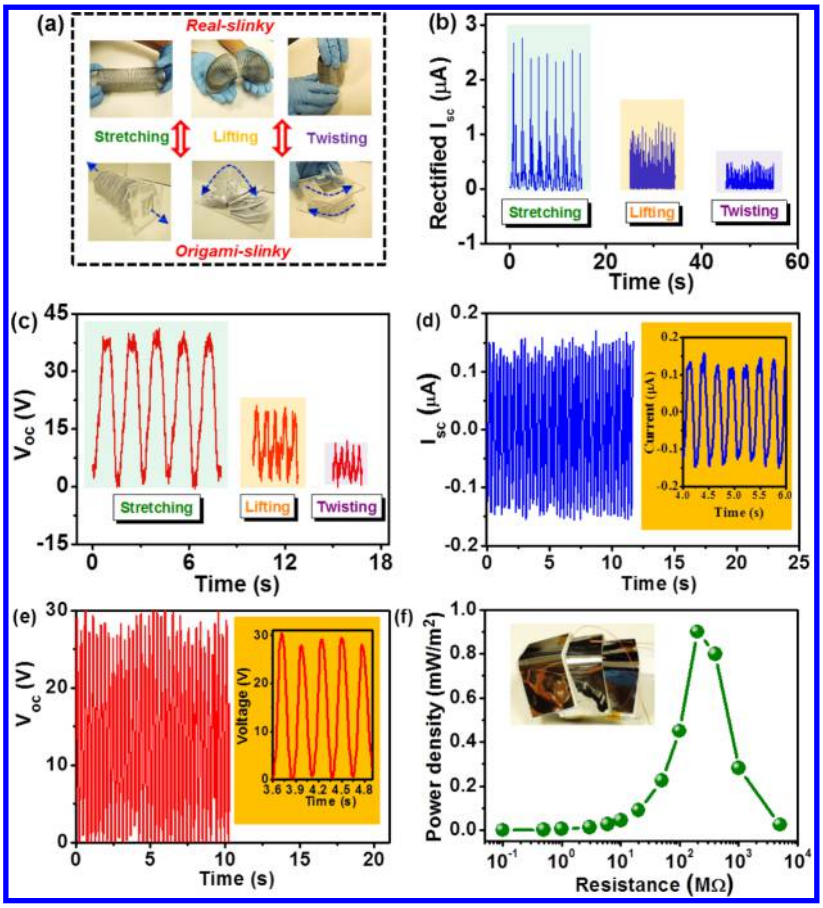

Figure 4. Mechanical energy harvester. (a) Realization of slinky motions by slinky TENG. (b) Rectified I_{sc} and (c) V_{oc} from various human motions of the slinky TENG. The inset images demonstrate the corresponding motions, where the arrows indicate the direction of applied force. (d) I_{sc} and (e) V_{oc} of the doodlebug TENG. The inset shows five enlarged cycles within the electrical output measurement. (f) Relationship between instantaneous power density and resistance of the external loads of the doodlebug TENG. The maximum power density reaches 0.9 mW m^{-2} when the external load is 200 MΩ. The inset image shows the photograph of the as-fabricated TENG.

active status of the device within the period of the measurements and applications.[26−28] Figure 1c,d shows the photographs of real devices, including a single unit cell and multiple units in parallel connection.

Figure 2 illustrates the working mechanism of the slinky TENG, which is operated in single-electrode mode.[29,30] At the original state (without external force), paper and the PTFE thin film are separated due to the stiffness of the paper substrate, and there is no electric output (Figure 2a). By applying an external force on the slinky TENG, paper and the PTFE thin film are contacted, which contribute to the charged surfaces of paper and the PTFE thin film (Figure 2b). Since PTFE is more triboelectrically negative than paper in the triboelectric series,[31] electrons will transfer from the paper surface to the surface of the PTFE thin film. After these two surfaces are separated, a potential difference will be formed between the paper and the PTFE thin film, causing electrons to flow from the Al foil to the ground (Figure 2c) and achieve equilibrium (Figure 2d). This is the half-cycle of slinky TENG operation.

Once the slinky TENG is pressed again, it will generate another potential difference, causing electrons to flow from the ground to the Al foil (Figure 2e) and finally achieve a new equilibrium (Figure 2f). This is the other half-cycle of the slinky TENG operation. If the slinky TENG is operated periodically, the electric output will be continuously provided.

To form a slinky TENG, each octagonally shaped unit can be easily connected *via* paper joints that are produced during origami folding without any extra wiring processes. As shown in Supporting Information Figure S1, the scheme clearly indicates how we connect individual unit cells into a parallel configuration. The image of joints also shows that the Al electrodes are separated and attached into each unit cell independently. Typical output characteristics of the slinky TENG were systematically investigated in Figure 3. V_{oc} and I_{sc} were measured to characterize the performance of the slinky TENG. Figure 3a,b displays the I_{sc} and V_{oc} of a single unit cell in the slinky TENG. The obtained I_{sc} and V_{oc} are 0.3 μA and 20 V, respectively. To further understand the dependence of electrical outputs on the number of units in a parallel connection, rectified I_{sc} of different number of units was measured in Figure 3c. It should be noted that the output current

is approximately linearly proportional to the number of connection units. When seven units are all set in a parallel connection, a rectified I_{sc} of 2 μA can thus be achieved. The transferred charge (ΔQ) of a different number of units is also shown in the inset. The maximum amount of transferred charge is 0.55 μC for seven units. In contrast, the V_{oc} of the entire TENG is not the sum but the equivalent to that in the individual unit. The rectified I_{sc} and V_{oc} of different connection series were investigated and is shown in Figure S2 (Supporting Information). One can see that the V_{oc} is almost identical regardless of the connection series, in contrast to the rectified I_{sc}. From the above-mentioned results, it is expected to enhance the electric output by incorporating more units while keeping the contact area of the TENG constant. Moreover, the stability of the electrode is one of the key issues that affect output characteristics of TENGs. As shown in Figure S3, the resistance distributions of Al foil on a paper substrate were measured after repeated pressing and releasing cycling tests. It is clear that the resistance distributions of Al foil remain stable with only negligible changes after 60 000 cycling tests. The results indicate excellent reliability of the Al foil on a paper substrate.

Resistors were utilized as external loads to further investigate electric outputs of the slinky TENG. As displayed in Figure 3d, the current amplitude drops with increasing load resistance due to the Ohmic loss, while the voltage follows a reverse trend. As shown in Figure 3e, the maximum instantaneous peak power density of seven units is 0.14 W m^{-2} at a load resistance of 400 MΩ. Figure 3f demonstrates the four commercial green LEDs driven by the slinky TENG. The observed bright green light emission indicates that these LEDs can be directly powered by pressing and releasing the as-fabricated TENG.

Additionally, the triggering frequency is another critical factor that could significantly affect the TENG's output.[32] The rectified I_{sc} of the slinky TENG under compressive force with different frequencies was investigated, as shown in Figure S4 (Supporting Information). As the frequency of the external force increases from 2.5 to 4.5 Hz, the rectified I_{sc} increases from 0.2 to 1.6 μA due to external electrons flowing to reach equilibrium in a shorter time. Meanwhile, toward large-scale application, the slinky TENG is fabricated into different contact areas shown in Figure S5 (Supporting Information). Figure S5a shows the rectified I_{sc} of the slinky TENG with different contact areas. One can see that the output current is monotonically increased with the contact area varied from 8 to 128 cm^2. Correspondingly, the instantaneous peak power density of the slinky TENG in different contact areas is shown in Figure S5b. The peak power density dramatically increases with the contact area, reaching 11 mW m^{-2} when the contact area equals 128 cm^2.

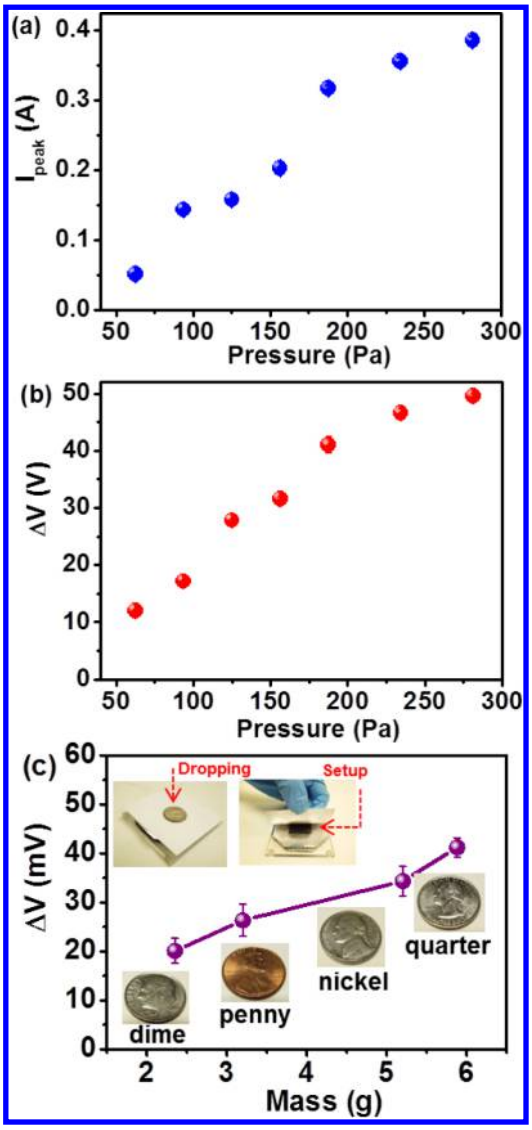

Figure 5. Self-powered pressure sensor. (a) Current response. (b) Voltage response under various forces induced by a linear motor. (c) Peak voltage (V_{peak}) responses of various types of coins were measured. Height of the drop is about 2 cm. The top inset images show the setup of a designed pressure sensor. The bottom inset images show the photographs of coins used.

To understand the effect of inducing origami configurations to TENGs, the slinky TENG is compared with a real metal slinky, which can realize various kinds of human motions, such as stretching, lifting, and twisting (Figure 4a). Figure 4b,c shows the typical electric outputs of the slinky TENG in harvesting various human motions, including I_{sc} and V_{oc}. A monotonical decrease observed in electrical outputs from stretching to twisting is due to the fact that the triboelectric outputs strongly depend on the distance of the gap created during mechanical motions.[33] The results indicate that the slinky TENG can effectively harvest ambient mechanical energy from various directions in contrast to the conventional TENG.

To further assess the applicability of the origami configuration in TENG technology, another famous

structure inside the scope of origami is implemented, which is named doodlebug TENG. Figure 4d,e displays the electric outputs of the doodlebug TENG, where the I_{sc} and V_{oc} are approximately 0.15 μA and 30 V, respectively. Figure 4f shows the maximum output power density of 0.9 mW m^{-2} at a load resistance of 200 MΩ. A photograph of the as-fabricated device based on doodlebug configuration is also shown as the inset. The results further point out the feasibility of utilizing diverse origami configurations in future TENG technology.

The TENG's electric output strongly depends on the external force, yielding higher output with larger force. Figure 5a,b displays the current and voltage response of the slinky TENG in a single unit cell under external force applied by a commercial linear motor. One can see that the electric outputs of the TENG increased upon increasing the applied pressure varied from 62.5 to 281.5 Pa. Specifically, the enhancement of electric outputs can be attributed to the increased contact areas by higher applied pressure between the PTFE thin film and the paper origami substrate, which is generally neither flat nor smooth. A larger contact force can reduce local gaps or voids introduced by surface roughness, substrate deformation, and contamination from the environment. Detailed information on the electric outputs with different applied force from the linear motor is also shown in (Supporting Information Figure S6).

The TENG itself can generate a voltage or current signal through contact electrification between two triboelectric materials by external mechanical forces, indicating its potential to be applied as a self-powered pressure sensor.[34] Here, with a simple design, a single unit cell is uniformly covered with a print paper on the top of its surface, and then standard coins are dropped from a fixed height to the central area of the cell. When a selected coin touched the surface, the gap between the PTFE and paper became narrow, leading to a detectable signal output. Figure 5c shows the voltage responses of a designed pressure sensor based on the slinky TENG. One can see that the TENG is able to detect the difference in mass from the output voltages. The individual signal output from dropping various types of coins is also shown in (Supporting Information Figure S7). The existing results reveal that our sensor can be well-utilized in our daily life.

Furthermore, for a pressure sensor application, it is of great importance to evaluate the sensitivity. Here, the relative sensitivity is defined as $(\Delta S/S_R)$, where sensitivity $(S) = (\Delta I/I_{off})/\Delta P$; ΔI is the relative change in current, I_{off} is the current of the sensor under no load, ΔP is the change in applied pressure, and S_R represents the sensitivity under applied pressure of 1562.5 Pa, which is set as the reference. As shown in Figure S8, slinky-like TENGs with multiple units and different contact areas are measured for their sensitivity under various applied pressure. One can see that only small fluctuations in sensitivity can be perceived for TENGs of different contact areas and number of units. The results indicate that the designed TENG has great potential for use as a pressure sensor that is highly adaptable to environments with diverse dimensions.

CONCLUSION

In summary, a low-cost, light-weight, and environmentally friendly paper-based TENG with origami configurations is demonstrated for harvesting ambient mechanical energy and serving as a self-powered pressure sensor. The dependence of electric outputs on the number of connection units and contact areas has been systematically studied. This prototype slinky TENG is able to provide an open-circuit voltage of 20 V and a short-circuit current of 2 μA. The corresponding peak power density is approximately 0.14 W m^{-2}, which is capable of lighting four LEDs simultaneously. Moreover, the slinky TENG can harvest energy from various kinds of human motions, indicating its multifunctionality in comparison with the conventional TENG. Furthermore, the slinky TENG can act as a self-powered pressure sensor to sense the difference in mass of standard coins. This study opens up the possibility of utilizing origami configuration into TENG design, extending its application scope, especially for paper-based portable power sources and pressure sensors.

METHODS

Fabrication of the Slinky TENG Unit. Normal printer paper with a thickness of 75 μm is selected as the substrate due to its low cost, flexibility, and light weight. The fabrication starts from cutting printer paper into square pieces with dimensions of 4 cm × 4 cm, 8 cm × 8 cm, and 16 cm × 16 cm. Then, each piece is folded into an "L" shape. Four L-shaped pieces are connected to yield one unit of the slinky TENG.

Assembly of Slinky TENG Units into a Slinky TENG. To assemble the slinky TENG, a 0.1 mm commercial aluminum coating foil (on moisture-resistant polyester) and 25 μm PTFE thin film with nanowire-like structure were sequentially adhered to the unit cell of the paper substrate by glue sticks. Before adhesion, to ensure perfect contact electrification, the PTFE thin film was first cleaned with isopropyl alcohol and deionized water. Second, the ICP reactive ion etching was applied to fabricate the nanowire-like structure on the PTFE surface where O_2, Ar, and CF_4 gases were implemented with a flow ratio of 10.0, 15.0, and 30.0 sccm, respectively. A large density of plasma was generated by a power source of 400 W. Another power source of 100 W was used to accelerate the plasma ions. Specifically, the PTFE film was etched for 40 s to get the nanowire-like structures with an average thickness of ~700 nm. Finally, a slinky-shaped device can thus be achieved by assembling a number of unit cells with proper adhesion processes. The conducting copper wires were also connected to the aluminum foils serving as electrodes for signal output.

Characterization. The surface morphology of the PTFE thin film was characterized by a Hitachi SU-8010. For the measurement of the electric outputs of the slinky TENG, an external force was applied by a commercial linear mechanical motor, and there would be friction between the PTFE thin film and paper, resulting in triboelectric potential and electric output in the external circuit. The open-circuit voltage was measured by using a Keithley 6514 system electrometer, while the short-circuit current was measured by using an SR570 low-noise current amplifier (Stanford Research System).

Conflict of Interest: The authors declare no competing financial interest.

Acknowledgment. Research was supported by U.S. Department of Energy, Office of Basic Energy Sciences under Award DEFG0207ER46394, NSF, and the Knowledge Innovation Program of the Chinese Academy of Sciences (Grant KJCX2-M13). P.-K.Y. thanks the Ministry of Science and Technology (103-2917-I-002-169), Taiwan, for support. Patents have been filed to protect the reported technologies.

Supporting Information Available: Additional information, figures, and tables. This material is available free of charge *via* the Internet at http://pubs.acs.org.

REFERENCES AND NOTES

1. Irimia-Vladu, M. "Green" Electronics: Biodegradable and Biocompatible Materials and Devices for Sustainable Future. *Chem. Soc. Rev.* **2014**, *43*, 588–610.
2. Hu, L. B.; Choi, J. W.; Yang, Y.; Jeong, S.; La Mantia, F.; Cui, L. F.; Cui, Y. Highly Conductive Paper for Energy-Storage Devices. *Proc. Natl. Acad. Sci. U.S.A.* **2009**, *106*, 21490–21494.
3. Yuan, L. Y.; Yao, B.; Hu, B.; Kuo, K. F.; Chen, W.; Zhou, J. Polypyrrole-Coated Paper for Flexible Solid-State Energy Storage. *Energy Environ. Sci.* **2013**, *6*, 470–476.
4. Yuan, L. Y.; Xiao, X.; Ding, T. P.; Zhong, J. W.; Zhang, X. H.; Shen, Y.; Hu, B.; Huang, Y. H.; Zhou, J.; Wang, Z. L. Paper-Based Supercapacitors for Self-Powered Nanosystems. *Angew. Chem., Int. Ed.* **2012**, *51*, 4934–4938.
5. Fang, Z. Q.; Zhu, H. L.; Yuan, Y. B.; Ha, D.; Zhu, S. Z.; Preston, C.; Chen, Q. X.; Li, Y. Y.; Han, X. G.; Lee, S.; Chen, G.; Li, T.; Munday, J.; Huang, J. S.; Hu, L. B. Novel Nanostructured Paper with Ultrahigh Transparency an Ultrahigh Haze for Solar Cells. *Nano Lett.* **2014**, *14*, 765–773.
6. Preston, C.; Fang, Z. Q.; Murray, J.; Zhu, H. L.; Dai, J. Q.; Munday, J. N.; Hu, L. B. Silver Nanowire Transparent Conducting Paper-Based Electrode with High Optical Haze. *J. Mater. Chem. C* **2014**, *2*, 1248–1254.
7. Zhong, Q.; Zhong, J.; Hu, B.; Hu, Q. Y.; Zhou, J.; Wang, Z. L. A Paper-Based Nanogenerator as a Power Source and Active Sensor. *Energy Environ. Sci.* **2013**, *6*, 1779–1784.
8. Hu, Q. Y.; Wang, B.; Zhong, Q.; Zhong, J. W.; Hu, B.; Zhang, X. Q.; Zhou, J. Metal-Free and Non-Fluorine Paper-Based Generator. *Nano Energy* **2014**, 10.1016/j.nanoen.2014.09.036.
9. Lin, L.; Jing, Q. S.; Zhang, Y.; Hu, Y. F.; Wang, S. H.; Bando, Y.; Han, R. P. S.; Wang, Z. L. An Elastic-Spring-Substrated Nanogenerator as an Active Sensor for Self-Powered Balance. *Energy Environ. Sci.* **2013**, *6*, 1164–1169.
10. Fan, F. R.; Tian, Z. Q.; Wang, Z. L. Flexible Triboelectric Generator. *Nano Energy* **2012**, *1*, 328–334.
11. Baland, J.; Chao, Y. H.; Suzuki, Y.; Tai, Y. C. Micro Electret Power Generator. In *Proceedings of the 16th IEEE International Conference on Micro Electro Mechanical Systems*; Kyoto, Japan, Januar 23, **2003**; pp 538−541.
12. Xie, Y.; Bos, D.; de Vreede, L. J.; de Boer, H. L.; van der Meulen, M.-J.; Versluis, M.; Sprenkels, A. J.; van den Berg, A.; Eijkel, J. C. T. High-Efficiency Ballistic Electrostatic Generator Using Microdroplets. *Nat. Commun.* **2014**, *5*, 3575–3580.
13. Lin, L.; Xie, Y. N.; Wang, S. H.; Wu, W. Z.; Niu, S. M.; Wen, X. N.; Wang, Z. L. Triboelectric Active Sensor Array for Self-Powered Static and Dynamic Pressure Detection and Tactile Imaging. *ACS Nano* **2013**, *7*, 8266–8274.
14. Lin, Z.-H.; Cheng, G.; Yang, Y.; Zhou, Y. S.; Lee, S.; Wang, Z. L. Triboelectric Nanogenerator as an Active UV Photodetector. *Adv. Funct. Mater.* **2014**, *24*, 2810–2816.
15. Lin, L.; Wang, S.; Xie, Y.; Jing, Q.; Niu, S.; Hu, Y.; Wang, Z. L. Segmentally Structured Disk Triboelectric Nanogenerator for Harvesting Rotational Mechanical Energy. *Nano Lett.* **2013**, *13*, 2916–2923.
16. Bai, P.; Zhu, G.; Lin, Z.-H.; Jing, Q.; Chen, J.; Zhang, G.; Ma, J.; Wang, Z. L. Integrated Multilayered Triboelectric Nanogenerator for Harvesting Biomechanical Energy from Human Motion. *ACS Nano* **2013**, *7*, 3713–3719.
17. Lin, Z.-H.; Zhu, G.; Zhou, Y. S.; Yang, Y.; Bai, P.; Chen, J.; Wang, Z. L. A Self-Powered Triboelectric Nanosensor for Mercury Ion Detection. *Angew. Chem., Int. Ed.* **2013**, *52*, 5065–5069.
18. Yang, W. Q.; Chen, J.; Jing, Q. S.; Yang, J.; Wen, X. N.; Su, Y. J.; Zhu, G.; Bai, P.; Wang, Z. L. 3D Stack Integrated Triboelectric Nanogenerator for Harvesting Vibration Energy. *Adv. Funct. Mater.* **2014**, *24*, 4090–4096.
19. Yang, W. Q.; Chen, J.; Zhu, G.; Yang, J.; Bai, P.; Su, Y. J.; Jing, Q. S.; Cao, X.; Wang, Z. L. Harvesting Energy from the Natural Vibration of Human Walking. *ACS Nano* **2013**, *7*, 11317–11324.
20. Mouthuy, P.-O.; Coulombier, M.; Pardoenm, T.; Raskin, J.-P.; Jonas, A. M. Overcurvature Describes the Buckling and Folding of Rings from Curved Origami to Foldable Tents. *Nat. Commun.* **2012**, *3*, 1290–1298.
21. Felton, S.; Tolley, M.; Demaine, E.; Rus, D.; Wood, R. A Method for Building Self-Folding Machines. *Science* **2014**, *345*, 644–646.
22. Nogi, M.; Komoda, N.; Otsuka, K.; Suganuma, K. Foldable Nanopaper Antennas for Origami Electronics. *Nanoscale* **2013**, *5*, 4395–4399.
23. Jung, Y.; Wang, X.; Kim, J.; Kim, S. H.; Ren, F.; Pearton, S. J.; Kim, J. GaN-Based Light-Emitting Diodes on Origami Substrates. *Appl. Phys. Lett.* **2012**, *100*, 231113.
24. Song, Z.; Ma, T.; Tang, R.; Cheng, Q.; Wang, X.; Krishnaraju, D.; Panat, R.; Chan, C. K.; Yu, H.; Jiang, H. Origami Lithium-Ion Batteries. *Nat. Commun.* **2014**, *5*, 3140–3146.
25. Scida, K.; Li, B.; Ellington, A. D.; Crooks, R. M. DNA Detection Using Origami Paper Analytical Devices. *Anal. Chem.* **2013**, *85*, 9713–9720.
26. Malecki, J. A. Linear Decay of Charge in Electrets. *Phys. Rev. B: Condens. Matter Mater. Phys.* **1999**, *59*, 9954–9960.
27. Xia, Z.; Gerhard-Multhaupt, R.; Kunstler, W.; Wedel, A.; Danz, D. High Surface-Charge Stability of Porous Polytetrafluoroethylene Electret Films at Room and Elevated Temperatures. *J. Phys. D: Appl. Phys.* **1999**, *32*, L83–L85.
28. Schwödiauer, R.; Bauer-Gogonea, S.; Bauer, S.; Heitz, J.; Arenholz, E.; Bäuerle, D. Charge Stability of Pulsed-Laser Deposited Polytetrafluoroethylene Film Electrets. *Appl. Phys. Lett.* **1998**, *73*, 2941–2943.
29. Yang, Y.; Zhou, Y. S.; Zhang, H. L.; Chen, J.; Liu, Y.; Lee, S. M.; Wang, Z. L. A Single-Electrode Based Triboelectric Nanogenerator as Self-Powered Tracking System. *Adv. Mater.* **2013**, *25*, 6594–6601.
30. Meng, B.; Tang, W.; Too, Z.-H.; Zhang, X.; Han, M.; Liu, W.; Zhang, H. A Transparent Single-Friction-Surface Triboelectric Generator and Self-Powered Touch Sensor. *Energy Environ. Sci.* **2013**, *6*, 3235–3240.
31. McCarty, L. S.; Whitesides, G. M. Electrostatic Charging Due to Separation of Ions at Interfaces: Contact Electrification of Ionic Electrets. *Angew. Chem., Int. Ed.* **2008**, *47*, 2188–2207.
32. Zhang, X. S.; Han, M. D.; Wang, R. X.; Zhu, F. Y.; Li, Z. H.; Wang, W.; Zhang, H. X. Frequency-Multiplication High-Output Triboelectric Nanogenerator for Sustainably Powering Biomedical Microsystems. *Nano Lett.* **2013**, *13*, 1168–1172.
33. Niu, S. M.; Wang, S. H.; Lin, L.; Liu, Y.; Zhou, Y. S.; Hu, Y. F.; Wang, Z. L. Theoretical Study of Contact-Mode Triboelectric Nanogenerators as an Effective Power Source. *Energy Environ. Sci.* **2013**, *6*, 3576–3583.
34. Fan, F. R.; Lin, L.; Zhu, G.; Wu, W.; Zhang, R.; Wang, Z. L. Transparent Triboelectric Nanogenerators and Self-Powered Pressure Sensors Based on Micropatterned Plastic Films. *Nano Lett.* **2012**, *12*, 3109–3114.